JOURNAL OF GENERAL VIROLOGY

RESEARCH ARTICLE

Ng *et al.*, *Journal of General Virology* 2021;102:001652

DOI 10.1099/jgv.0.001652

MICROBIOLOGY SOCIETY

OPEN ACCESS

Plasticity of the lettuce infectious yellows virus minor coat protein (CPm) in mediating the foregut retention and transmission of a chimeric CPm mutant by whitefly vectors

James C. K. Ng[1,2,*,†], James H. C. Peng[1†], Angel Y. S. Chen[1], Tongyan Tian[3], Jaclyn S. Zhou[1] and Thomas J. Smith[4]

Abstract

Transmission of the crinivirus, lettuce infectious yellows virus (LIYV), is determined by a minor coat protein (CPm)-mediated virion retention mechanism located in the foregut of its whitefly vector. To better understand the functions of LIYV CPm, chimeric CPm mutants engineered with different lengths of the LIYV CPm amino acid sequence and that of the crinivirus, lettuce chlorosis virus (LCV), were constructed based on bioinformatics and sequence alignment data. The 485 amino acid-long chimeric CPm of LIYV mutant, CPmP-1, contains 60% (from position 3 to 294) of LCV CPm amino acids. The chimeric CPm of mutants CPmP-2, CPmP-3 and CPmP-4 contains 46 (position 3 to 208), 51 (position 3 to 238) and 41% (position 261 to 442) of LCV CPm amino acids, respectively. All four mutants moved systemically, expressed the chimeric CPm and formed virus particles. However, following acquisition feeding of the virus preparations, only CPmP-1 was retained in the foreguts of a significant number of vectors and transmitted. In immuno-gold labelling transmission electron microscopy (IGL-TEM) analysis, CPmP-1 particles were distinctly labelled by antibodies directed against the LCV but not LIYV CPm. In contrast, CPmP-4 particles were not labelled by antibodies directed against the LCV or LIYV CPm, while CPmP-2 and -3 particles were weakly labelled by anti-LIYV CPm but not anti-LCV CPm antibodies. The unique antibody recognition and binding pattern of CPmP-1 was also displayed in the foreguts of whitefly vectors that fed on CPmP-1 virions. These results are consistent with the hypothesis that the chimeric CPm of CPmP-1 is incorporated into functional virions, with the LCV CPm region being potentially exposed on the surface and accessible to anti-LCV CPm antibodies.

INTRODUCTION

The genus *Crinivirus* (family *Closteroviridae*) comprises members that are disease causal agents of a wide range of economically important plant species, coinciding with the polyphagous nature of the different but distinct whitefly vectors (of the genera *Bemisia* and/or *Trialeurodes*) that transmit them. Whitefly transmission of criniviruses is achieved in a non-circulative, semi-persistent (NCSP) manner, a mode of transmission where the passage of virus through the vector's digestive and circulatory systems is not required for transmission, and the duration in which a vector remains viruliferous ranges from hours to days. Criniviruses are restricted to the phloem of infected plants, allowing them to be effectively acquired or inoculated by whitefly vectors during phloem feeding [1]. The mechanism underlying the NCSP transmission of criniviruses is far from elucidated. Most of our current knowledge on the molecular and biochemical determinants of crinivirus transmission has been obtained

Received 24 February 2021; Accepted 16 July 2021; Published 08 September 2021

Author affiliations: [1]Department of Microbiology and Plant Pathology, University of California, Riverside, CA 92521, USA; [2]Center for Infectious Disease and Vector Research, University of California, Riverside, CA 92521, USA; [3]California Department of Food and Agriculture, Sacramento, CA 95832, USA; [4]Department of Biochemistry and Molecular Biology, University of Texas Medical Branch at Galveston, TX, 77555, USA.

***Correspondence:** James C. K. Ng, jamesng@ucr.edu

Keywords: crinivirus; foregut; lettuce chlorosis virus; lettuce infectious yellows virus; retention; transmission; whitefly.

Abbreviations: AAP, acquisition access period; BYV, beet yellows virus; BYVaV, blackberry yellow vein associated virus; CCYV, cucurbit chlorotic yellows virus; CP, major coat protein; CPm, minor coat protein; CTV, citrus tristeza virus; CYSDV, cucurbit yellow stunting disorder virus; HSP70h, heat-shock protein 70 homolog; IGL-TEM, immuno-gold labelling transmission electron microscopy; LCV, lettuce chlorosis virus; LIYV, lettuce infectious yellows virus; MEAM1, Middle East–Asia Minor 1; NCSP, non-circulative, semi-persistent; NOS, nopaline synthase; nt, nucleotide; NW, New World; ORFs, open reading frames; PepMV, pepino mosaic virus; SPaV, strawberry pallidosis associated virus; SPCSV, sweet potato chlorotic stunt virus; ToCV, tomato chlorosis virus; TuMV, turnip mosaic virus; VR, virion retention; WT, wild type.

†These authors contributed equally to this work

Four supplementary tables and two supplementary figures are available with the online version of this article.

through studies of lettuce infectious yellows virus (LIYV), although much more still remains to be discovered.

LIYV is the type species of the genus *Crinivirus*. As with most other crinviruses, its genome is made up of two single-stranded, positive-sense RNAs. The 8117 nucleotide (nt)-long RNA 1 encodes proteins associated with viral replication [2, 3], while the 7193 nt-long RNA 2 contains open reading frames (ORFs) encoding proteins that have been demonstrated or implicated to be involved in various viral functions [4–9]. Of these proteins, five – p5, HSP70h (a heat-shock protein 70 homologue), p59, CP (major coat protein) and CPm (minor coat protein) – are encoded by a quintuple gene block, designated the 'hallmark closterovirus gene array'. Both LIYV genomic RNAs are individually encapsidated into flexuous filamentous (~750×12 nm) particles [10, 11]. Immuno-gold labelling transmission electron microscopy (IGL-TEM) analysis of LIYV virions has shown that an antibody directed against the LIYV CP exhibits an affinity for its target antigen located nearly throughout the entire length of the virion, whereas the antigen target of the anti-LIYV CPm antibody is only present on one end (the 'tail') of the virion [10]. For two members of the family *Closteroviridae*, citrus tristeza virus (CTV) and beet yellows virus (BYV), interactions between CPm and HSP70h, along with p61 or p64 (the homologues of LIYV p59 in CTV and BYV, respectively) are responsible for the tail formation of the virion [12, 13]. In the case of LIYV, although HSP70h and p59 have been detected in virion preparations, their locations on the virion have not been positively identified [10].

LIYV is transmitted exclusively by the New World (NW) species of *Bemisia tabaci* (order: Hemiptera; family: Aleyrodidae) whitefly vector using a retention mechanism that facilitates the binding of virions to the vector's foregut [4]. When vectors that fed on stretched parafilm membrane containing artificial diet augmented with LIYV virions were examined by immunofluorescent localization, also referred to as a virus or virion retention (VR) assay, a significant number were found to retain the virions in their foreguts. Correspondingly, transmission was observed when vectors that fed on the LIYV virion-augmented artificial diet were allowed inoculation access feeding on lettuce seedlings. In contrast, a significantly reduced number of non-vector *B. tabaci* Middle East–Asia Minor (MEAM) 1 species retained virions in their foreguts and no corresponding virus transmission was observed [4]. Two additional studies have provided clear evidence that LIYV CPm is a major determinant of virion retention and transmission by the NW vector. First, retention assays using bacterial-expressed recombinant (*r*) LIYV capsid proteins (CP, CPm, HSP70h and p59) showed that a significant number of vectors that fed on *r*CPm harboured fluorescent signals in their foreguts compared to those that fed the other three recombinant capsid proteins [4]. Second, virus retention and transmission (VRT) assays performed using a transmission-defective LIYV CPm mutant and the CPm restored virus (see details in the next paragraph) demonstrated that only the latter was retained in the foreguts of a significant number of vectors and transmitted. Studies demonstrating the foregut retention and transmission of cucurbit chlorotic yellows virus by the *B. tabaci* Mediterranean (MED) species [14] support the notion that the transmission of other criniviruses is also mediated by a foregut retention process. Thus, the CPm of other criniviruses may likely play a similar role to LIYV CPm in the mediation of virion retention and transmission.

The structure of LIYV CPm has not yet been determined, making it challenging to engineer targeted mutations aimed at identifying the amino acid determinants of virion retention and transmission. A natural LIYV mutant with truncated CPm (1-5b) systemically infected *Nicotiana benthamiana* plants and formed virus particles. However, 1-5b was poorly retained in the vector's foregut compared to 1-5bM1, the CPm-restored virus. Correspondingly, vectors failed to transmit 1-5b, but transmitted 1-5bM1 at levels similar to those of wild-type (WT) LIYV [4, 9]. Further attempts at engineering truncations in the LIYV CPm have all resulted in mutants that were biologically active in plants but were transmission defective [1] (Chen *et al.*, unpublished data). The negative transmission results were difficult to interpret as they could be associated with defects in encapsidation and/or foregut retention. Given this context, the availability of functional mutants would be of great value in elucidating the CPm-mediated transmission mechanism of LIYV.

In this work, we first took a bioinformatics approach to analyse the crinivirus CPm, primarily focusing on LIYV and lettuce chlorosis virus (LCV), two criniviruses that infect lettuce plants and are transmitted by the NW vector. The analysis revealed a modest but intriguing similarity between a region in the N-terminus of LCV CPm and two laminin alpha chains. We then used the information to generate LIYV constructs engineered with specific chimeric LIYV–LCV CPms. Using the infectious cDNA clones of these chimeric constructs, we identified a functional LIYV mutant capable of foregut retention and transmission by whitefly vectors. Furthermore, the chimeric LIYV virions exhibited a unique recognition pattern in their interaction with antibodies directed against the anti-LIYV CPm and anti-LCV CPm, differing from that observed for WT (LIYV and LCV) virions. Together, these results demonstrate for the first time that LIYV CPm possesses novel functional plasticity in its role as determinant of virion retention and transmission by whitefly vectors.

METHODS

Bioinformatics analysis

Protein structure homology modelling was performed using the Swiss-Model server, available online at https://swiss-model.expasy.org [15], and the Phyre^2 web portal for protein modelling, prediction and analysis available online at http://www.sbg.bio.ic.ac.uk/phyre2 [16]. The secondary structures of LIYV and LCV CPm were predicted by the GOR IV secondary structure prediction method (https://npsa-prabi.ibcp.fr) [17]. Amino acid sequences were aligned using the Geneious Prime program (Biomatters, Ltd, Auckland, New Zealand). The accession numbers of the amino acid sequences used for alignment analysis are SIW59152.1 [cucurbit

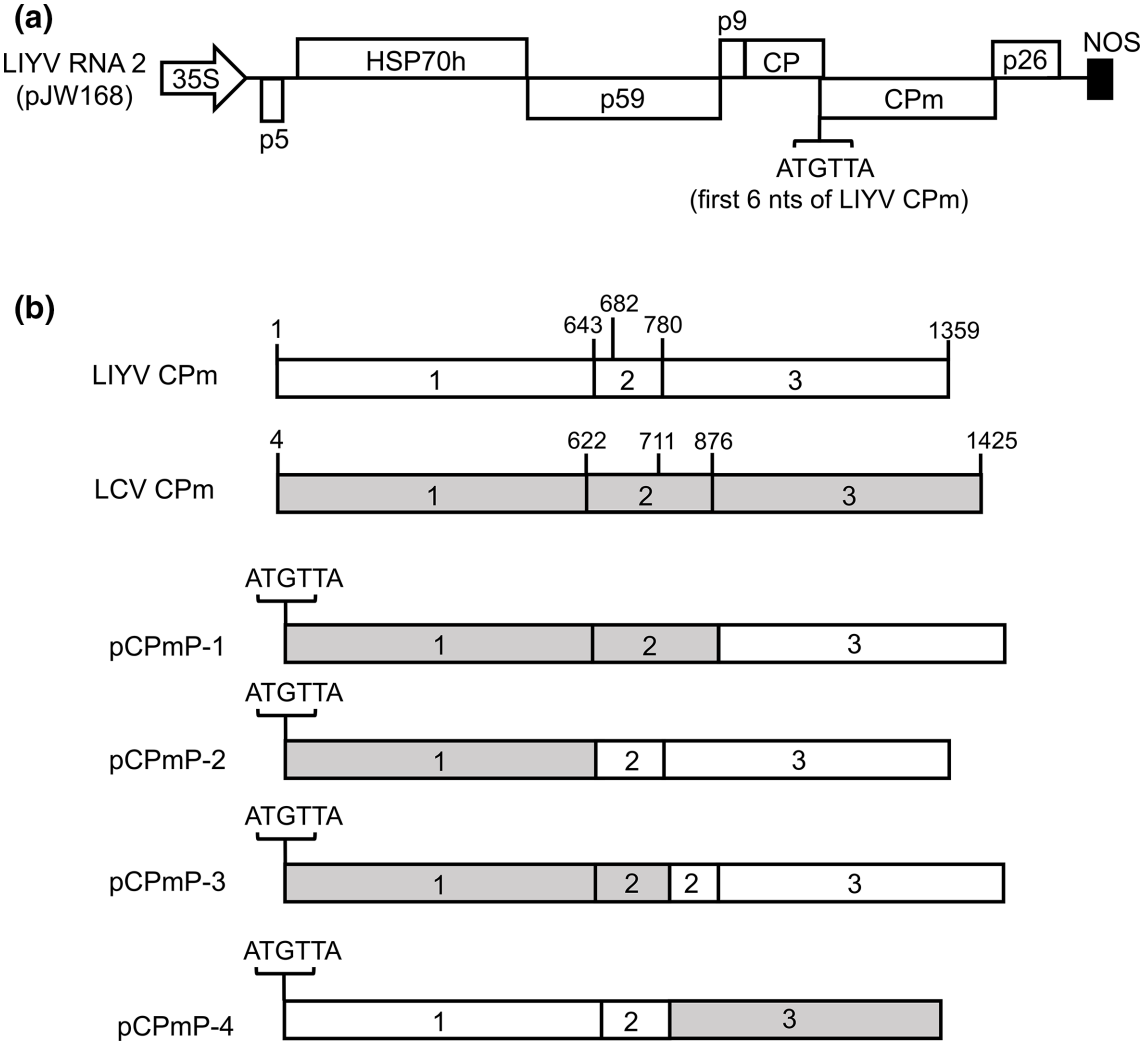

Fig. 1. Schematic diagrams of the cDNA clone of lettuce infectious yellow virus (LIYV) RNA 2 and the modifications engineered in its minor coat protein (CPm). (a) A map of the infectious cDNA clone of LIYV RNA 2 (pJW168) illustrating its genomic organization. White boxes represent open reading frames (ORFs) encoding the named proteins. The block arrow and black box indicate the locations of the cauliflower mosaic virus 35S promoter and the nopaline synthase terminator (NOS), respectively. (b) The chimeric CPm of four LIYV RNA 2 constructs engineered with partial-length LCV CPm sequences. The ORFs of LIYV CPm and LCV CPm are represented by white and grey boxes, respectively, and are demarcated into three regions, labelled '1', '2' and '3', based on the results of the bioinformatics analysis (see Fig. 2). Numbers above the LIYV CPm and LCV CPm ORFs mark the nt positions of the boundaries of the three demarcated regions. The nt sequences of region 2 located between nt 643 and 780 (for LIYV CPm) and between nt 622 and 876 (for LCV CPm) encode amino acids that are predicted to make up the longest random coil in these proteins (see Fig. 2). Constructs pCPmP-1, -2, -3 and -4 were engineered in the pJW168 backbone. Each construct was engineered with a different combination or arrangement of regions 1, 2 and 3 derived from the LCV and LIYV CPms as shown. The 5′ end of the chimeric CPm coding sequences of all four constructs begin with the first 6 nt (ATGTTA) of the LIYV CPm. Region 2 in pCPmP-3 is made up of a combination of the partial sequences from region 2 of LCV CPm (nt 622–711; grey) and LIYV CPm (nt 682–780; white).

chlorotic yellows virus (CCYV) CPm], AAP33616.1 [cucurbit yellow stunting disorder virus (CYSDV) CPm], CDG34561.1 [tomato chlorosis virus (ToCV) CPm], CAD21950.1 [sweet potato chlorotic stunt virus (SPCSV) CPm], AAV40971.1 [blackberry yellow vein associated virus (BYVaV) CPm], AAS79681.1 [strawberry pallidosis associated virus (SPaV) CPm], YP_003002363.1 (LCV CPm), NP_619697 (LIYV CP) and NP_619698 (LIYV CPm). The LIYV CPm sequence used for alignment was an updated version of the sequence represented by NP_619698.

Engineering of chimeric CPm constructs

A chimeric region consisting of the first six nucleotides of the LIYV CPm sequence (Fig. 1a) and the full-length LCV CPm coding sequence was generated by overlapping PCR using pJW168 (a binary plasmid harbouring the cDNA of WT

LIYV RNA 2) [18] and p35SLCVRNA2 (the binary plasmid containing the cDNA of WT LCV RNA2) [19] as templates. The PCR product was cloned to generate a plasmid named pCPmF-1. cDNA corresponding to chimeric sequences made up of partial-length LCV CPm and LIYV CPm sequences for making the constructs, pCPmP-1, pCPmP-2, pCPmP-3 and pCPmP-4, were obtained by overlapping PCRs using pCPmF-1 and pJW168 as templates. Each of the products obtained from the overlapping PCRs was digested with Hpa I and Nsi I and ligated to the vector backbone of similarly digested pJW168 to generate the final constructs (Fig. 1b). Information on the oligo primers used for PCR amplifications are provided in Table S4.

All PCR amplifications were performed using Herculase II Fusion DNA polymerase (Agilent Technologies). Following transformation in *Escherichia coli* strain DH5α and plasmid purification using the QIAprep Spin Miniprep kit (Qiagen), all plasmids containing cloned PCR amplified fragments were sequenced to ensure the absence of spurious mutations.

Transformation of *Agrobacterium* and agroinoculation

Binary plasmids of WT LIYV and LCV, as well as of all engineered CPm mutants, were transformed into *Agrobacterium tumefaciens* strain GV3101 using the freeze and thaw method [19]. The procedure for the growth and preparation of transformed *Agrobacterium* cultures was as previously described [18], except that the cultures were resuspended in activation buffer (10 mM $MgCl_2$, 10 mM MES and 150 µM acetosyringone) to an OD_{600} value of 0.25. Transgenic *N. benthamiana* plants expressing turnip mosaic virus (TuMV) HC-Pro (kindly provided by Bryce Falk, UC Davis) were used for agroinfiltration to enhance viral infection. Plants were grown to a stage with five–six fully expanded leaves before being used for agroinoculation. Leaves were co-infiltrated with *Agrobacterium* cultures containing pJW100 (a binary plasmid of WT LIYV RNA 1) and WT LIYV RNA 2 (pJW168) or mutant LIYV RNA 2 (engineered with chimeric CPm sequences). Viral infection in plants was determined based on symptom development and RT-PCR [9] at approximately 5–6 weeks-post-inoculation (p.i.). To facilitate WT LCV infection, leaves were co-infiltrated with *Agrobacterium* cultures containing p35SLCVRNA1 and p35SLCVRNA2 and infection was confirmed by symptom development and RT-PCR [19].

Virion purification, immunoblot analysis and IGL-TEM

Systemic leaves of infected plants collected at 6–7 weeks p.i. were used for virion purification. The procedures for virion preparation and quantification were described previously [9], except that virions or virus particles purified for acquisition feeding by whitefly vectors were resuspended in a 1× artificial diet [15% sucrose, 1% BSA in 1× TE (10 mM Tris-HCl, 1 mM EDTA, pH7.4)] [4]. The concentrations of virion preparations were determined by densitometry of the colloidal Coomassie blue-stained CP resolved in SDS-polyacrylamide gel [20]. Virion preparations were analysed by immunoblot analysis [4] using the antibodies against the LIYV CP, LIYV CPm and LCV CP at dilutions of 1:1500, as well as the antibody against the LCV CPm at a dilution of 1:500. IGL-TEM was performed as previously described [9].

Whitefly maintenance, VRT assays and statistical analysis

Non-viruliferous whitefly (*B. tabaci* NW) colonies were maintained on lima bean (*Phaseolus lunatus*) [4] or turnip (*Brassica rapa*) plants. VRT assays were performed essentially according to the procedure described by Chen *et al*. [4] with some modifications. Because whiteflies do not feed well and suffer high mortality on *N. benthamiana* plants, performing the assays using agroinfiltrated *N. benthamiana* plants as the source of virus acquisition has never been a favoured option. Instead, virus acquisition is achieved by membrane feeding [20]. In all our previous studies, we have not seen any negative effects of membrane feeding on whiteflies and their ability to acquire virus. Approximately 250 adult whiteflies were confined in a cage and fed (by membrane feeding) artificial diet alone or artificial diet containing purified virion preparations. Following an acquisition access period (AAP) of 14–16 h, half of the whiteflies were transferred from the cage to an uninfected lettuce seedling to determine virus transmissibility. Transmission was scored by symptom development and confirmed by RT-PCR. The remaining whiteflies from the same cage were subjected to the first clearing step of the virion retention assay in which they were fed artificial diet alone for an AAP of 6 h to flush out unbound virions or virus particles. Afterwards, the whiteflies were given a 16 h AAP to feed on artificial diet containing one of the following primary antibodies: a 1:600 dilution of an anti-LIYV virion IgG stock of 2 mg ml^{-1}, a 1:600 dilution of an anti-LIYV CPm IgG stock of 2 mg ml^{-1}, or a 1:1200 dilution of an anti-LCV CPm IgG stock of 4 mg ml^{-1}. This was followed by feeding the whiteflies artificial diet containing a 1:200 dilution of an Alexa Fluor 488-conjugated goat-anti-rabbit IgG [the secondary (detecting) antibody] for an AAP of 8 h. Finally, the whiteflies were subjected to a second clearing step in which they were fed artificial diet alone for an overnight AAP to flush out unbound or non-specifically bound ligands. There were some variations in the duration of the AAP in specific steps of the retention assay for the CPmP-1 virions. In experiment 1, following virion acquisition, whiteflies were not fed artificial diet in the first clearing step, i.e. there was no AAP. In experiment 4, whiteflies were given a 10 h AAP for the first clearing step and a 6 h AAP for the acquisition of the secondary antibody. However, these AAP variations were applied to all treatments (i.e. WT, mutant and diet control) in these experiments.

At the end of the virion retention assays, the heads of whiteflies were dissected and observed under a Nikon Labophot fluorescence microscope fitted with FITC/CY3 double

bandpass filters. The images of whiteflies' heads were taken using a Canon EOS T5i digital single-lens reflex camera. The results of virus retention in the foreguts of whitefly vectors were analysed by an unpaired two-tailed *t*-test for data that meet the requirements of normality and homogeneity of variances, or the Mann–Whitney test and presented in graphs using GraphPad Prism software (GraphPad Software, Inc., La Jolla, CA, USA). Virus transmissibility was determined by symptom development and/or by RT-PCR using the total RNA extracted from target lettuce plants [9]. Transmission results, where applicable, were analysed using a two-sided Fisher exact test in GraphPad Prism software.

RNA isolation, RT-PCR and nucleotide sequencing of chimeric CPmP-1 mutant

Total RNA from the systemic leaves of agroinoculated plants and the target plants used for virus transmission studies were extracted by the TRIzol method (Thermo Fisher Scientific). The first-strand cDNA, synthesized by reverse transcription using MMLV reverse transcriptase (Promega) and the LIYV 73-like (5′-CTCTTTATCATAGTCGCATGTGG-3′) primer, was used as a template for PCR amplification. Primer pairs LIYV 10-like (5′-CAAGCATTATGCAAAGGTGAAG-3′) and LIYV 73-like were used to PCR-amplify the CPm region in the first-strand cDNA using *Taq* DNA polymerase. Virion (v)RNA was isolated from the virion preparations of CPmP-1 using the Trizol LS reagent (Thermo Fisher Scientific) according to manufacturer's recommendation. The first strand of cDNA was generated from the vRNA using Maxima H Minus reverse transcriptase (Thermo Fisher Scientific) and LIYV 5 primer (5′-ATTCAATCACCACTCTCTGAT-3′). Next, the region containing the coding sequences of CP and CPm (2372 bp) were PCR-amplified by Herculase II DNA polymerase using the LIYV 6 and LIYV 13 primers [21]. The PCR products were cloned into the pGem T Easy vector and transformed in *E. coli* DH5α, and individual clones were randomly selected for DNA sequencing confirmation.

RESULTS

Bioinformatics analysis of CPm

The CPm of LIYV and LCV share a low primary sequence homology (with 20.5% identity and 39.3% similarity). When both sequences were analysed by the Swiss-Model tool for homology-based structure prediction, only weak homology was found to known protein structures. The top hit for LIYV CPm was the coat protein (CP) of the filamentous pepino mosaic virus (PepMV; genus *Potexvirus*) (SMTL ID: 5fn1.1) [22] with 14.79% identity (28% similarity) and 31% coverage towards the distal one-third (C-terminus) of the target (Fig. 2a). The PepMV CP was the best match for LCV CPm as well, with 16.78% identity (29% similarity) and 31% coverage also towards the distal one-third (C-terminus) of the target (Fig. 2a). An interesting hit for LCV CPm was laminin subunit alpha-1 chain, domains LG4–5 (α1LG4-5) (SMTL ID: 2JD4.1) [23], with a 12.33% identity (27% similarity) and 31% coverage towards the proximal one-third (N-terminus) of the target (Fig. 2a). Laminins are a family of multidomain glycoproteins that play important roles in cell–extracellular matrix adhesion in invertebrates and for the assembly of the basal lamina in vertebrates [24]. An analysis using the Phyre^2 server predicted the N-terminus of LCV CPm and those of other criniviruses to also show low sequence identity when compared with α1LG4-5 (library ID: c2jd4B) (Table S1, available in the online version of this article), as well as with laminin subunit alpha-2 chain, domains LG4–5 (α2LG4-5) (library ID: c1okqA) [25] (Table S2). By contrast, LIYV CPm showed no structural homology with α1LG4-5 or any other laminin subunits. The possible implications of these predictions are provided in the discussion section.

The CPm sequences of LIYV and LCV were next subjected to secondary structure prediction using the GOR4 program, which predicted 27.65% helical content, 48.89% random coil and 23.45% extended strand in LIYV CPm and 20.25% helical content, 56.75% random coil and 23% extended strand in LCV CPm. An unstructured region of significant size (46 amino acids; from position 215 to 260) was the longest random coil predicted in LIYV CPm (Fig. 2a). In LCV CPm, the longest unstructured region, predicted to begin at position 208 and consisting of 85 amino acids (ending at position 292), was about double the size of that of LIYV CPm (Fig. 2a). The 46 amino acid random coil separated LIYV CPm into two regions in which the C-terminal region corresponded to the distal one-third that aligned with the PepMV CP in the Swiss-Model analysis (Fig. 2a). Likewise, the 85 amino acid random coil separated LCV CPm into two regions; here, the N-terminal (proximal) and C-terminal (distal) one-third regions corresponded to that aligned with laminin subunit alpha-1 chain, domains LG4–5 and the PepMV CP, respectively, in the Swiss-Model analysis (Fig. 2a).

A multiple sequence alignment of the full-length LIYV CP and that of the CPm encoded by eight individual criniviruses showed that the best homology was found in the distal one-half (C-termini) of the CPm sequences (Fig. 2b). The same alignment pattern was also observed when the full-length CP and CPm sequences of multiple criniviruses were compared (Fig. S1). A prominent feature seen in these alignments was the perfectly aligned S, R and D residues, invariant among all filamentous virus coat proteins [26]. The results were consistent with those obtained by Klaassen *et al.* [27] for the alignment of the LIYV CPm and CP sequences and the CP sequences of citrus tristeza virus and beet yellows virus, suggesting that the C-terminal one-half of the crinivirus CPm contained a duplicate copy of the CP. This possibility, coupled with the fact that both the CP and CPm are present on the virion capsid [10], points to the C-terminus as one region in the CPm that might be relatively necessary for capsid function.

Whiteflies retain and transmit LIYV virions engineered with a chimeric partial-length LCV CPm

Based on the protein prediction and amino acid sequence alignment results from the preceding section, we posited that

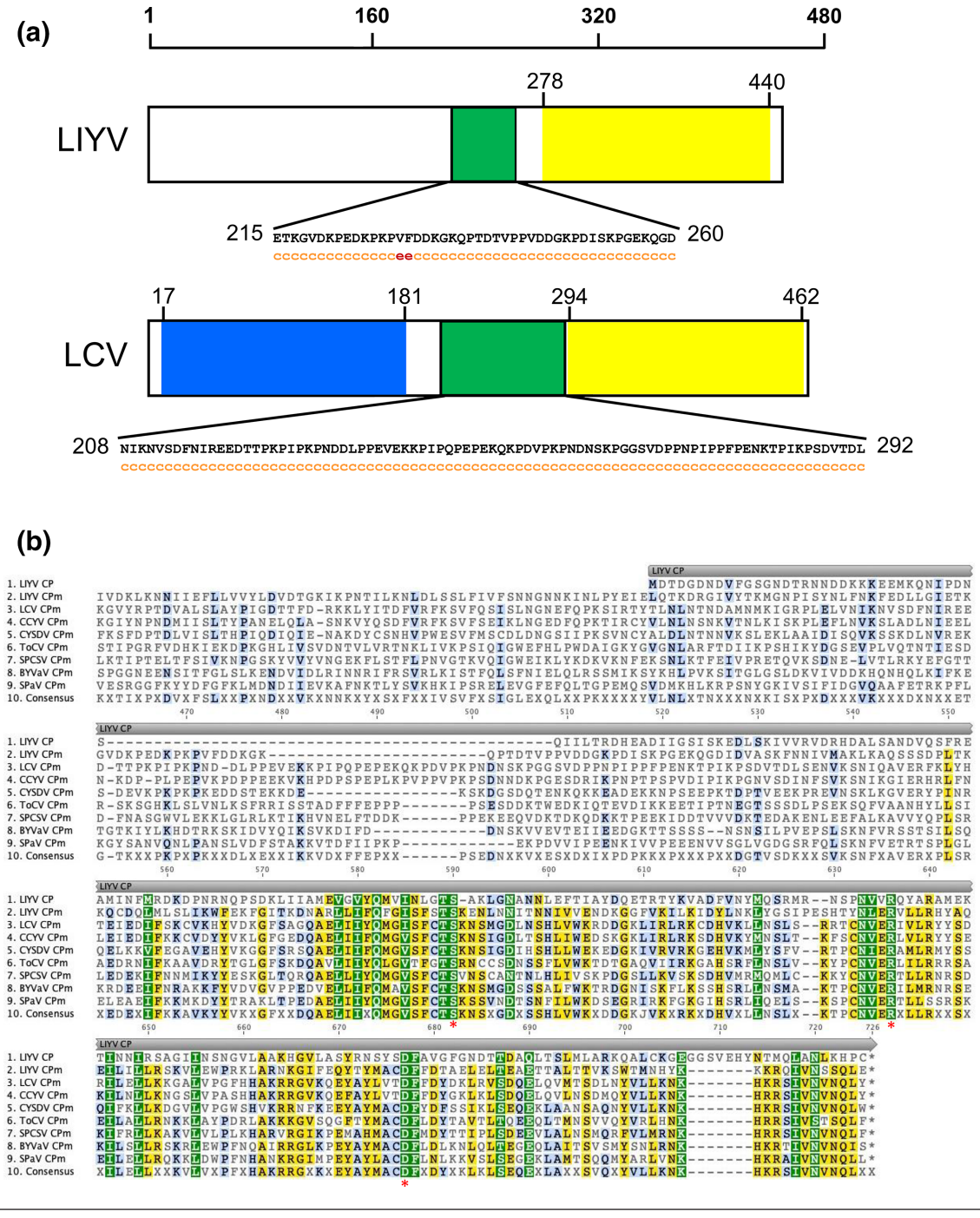

Fig. 2. Bioinformatics analysis of LIYV CPm and LCV CPm. (a) The genetic maps of full-length LIYV CPm (top) and LCV CPm (bottom) are shown with markings that depict the results obtained from the bioinformatics analysis performed in this study. The distal one-third (C-termini; yellow) of the CPm of both viruses corresponds to the regions in which the amino acids are aligned with those of PepMV coat protein predicted in Swiss-Model. The proximal one-third (N-terminus; blue) of the LCV CPm corresponds to the region in which the amino acids are aligned with those of laminin subunit alpha-1 chain, domains LG4–5 predicted in Swiss-Model. Green boxes correspond to the unstructured regions [46 amino acid (position 215–260) and 85 amino acid (position 208–292)] of LIYV CPm and LCV CPm, respectively, as predicted by the GOR4 program. c, random coil, e, extended strand. The numerical scale bar (with amino acid residue numbers) above the genetic maps serves as a guide to the relative sizes of the two CPms. (b) Multiple sequence alignment of the amino acid sequence of full-length LIYV CP and that of the CPm of eight criniviruses. The CPm sequences are truncated to allow for better visualization of the alignment. The homology of amino acids is depicted as follows: green, identical; yellow, 80–100% similar; light blue, 60–80% similar; white, <60% similar. The amino acids (S, R and D) conserved among the coat proteins of filamentous plant viruses [26] are marked by red asterisks.

the N-terminal one-half, or part thereof, of the crinivirus CPm could, in addition to capsid function, be involved in other roles such as transmission by whitefly vectors. To test this hypothesis, we engineered four LIYV mutant constructs with partial-length LCV and LIYV CPm sequences, from here on referred to as chimeric partial-length LCV CPm (CPmP) mutants, using pJW168 (a binary plasmid containing the cDNA of WT LIYV RNA2): pCPmP-1, which contained the LCV CPm coding sequence from position 4 to 876 and the LIYV CPm coding sequence from position 781 to 1359; pCPmP-2, which contained the LCV CPm coding sequence from position 4 to 621 and the LIYV CPm coding sequence from position 643 to 1359; pCPmP-3, which contained the LCV CPm coding sequence from position 4 to 711 and the LIYV CPm coding sequence from position 682 to 1359; and pCPmP-4, which contained the LIYV CPm coding sequence from position 1 to 780 and the LCV CPm coding sequence from position 877 to 1425 (Fig. 1). Region 1 in pCPmP-1,-2 and -3 began with the six nucleotides, ATGTTA, of the LIYV CPm coding sequence followed by the nucleotide at position 4 of the LCV CPm coding sequence (Fig. 1). ATGTTA could not be removed from these constructs as they also belong to the upstream ORF encoding the LIYV CP. Transgenic *N. benthamiana* plants expressing TuMV HC-Pro were infiltrated with *Agrobacterium* transformed with pJW100, a binary plasmid containing the cDNA of LIYV RNA 1 [18], along with *Agrobacterium* transformed with each of the chimeric CPmP (LIYV RNA 2) constructs or pJW168 (WT LIYV RNA 2). Viral infection, confirmed by RT-PCR, was observed in the systemic leaves of plants agroinfiltrated with the WT constructs as well as in those of plants agroinfiltrated with each of the chimeric constructs (Fig. 3a).

Virus purification was performed, and the resulting virion preparations were analysed by immunoblotting using polyclonal antibodies directed against LIYV CP, LIYV CPm, or LCV CPm (Fig. 3). As expected, the anti-LIYV CP antibody identified a 28 kDa protein corresponding to the molecular mass of the LIYV CP in the WT LIYV preparation as well as in the preparations of all four chimeric CPmP mutants (Fig. 3b). Both the anti-LIYV CPm and anti-LCV CPm antibodies also identified proteins with molecular masses of approximately 55.6, 51.2, 55 and 51 kDa, which corresponded to that expected for the chimeric CPm of mutants CPmP-1, -2, -3 and -4, respectively (Fig. 3c, d). The anti-LIYV CPm, but not the anti-LCV CPm, antibody identified WT LIYV CPm (Fig. 3c, d), indicating that they were specific to their target antigens.

The purified virion preparations were subjected to VRT assays using *B. tabaci* NW vectors. The presence of virions in the vector's foregut was determined using antibodies directed against the LIYV virion [4]. Five biological repeats of the VRT assay were performed using the preparations of CPmP-1, WT LIYV and diet-only control. The VR assays revealed that fluorescent signals were observed in an average of 15% (based on a cumulative total of 247/1674) of the foreguts of vectors that fed on the CPmP-1 preparations (at concentrations ranging from 182 to 801 ng μl^{-1}) (Fig. 4a, b). This retention result was not significantly different from the average of 18% (based on a cumulative total of 289/1553) of foreguts found to contain fluorescent signals for vectors that fed on the WT LIYV preparations (at concentrations ranging from 390 to 1945 ng μl^{-1}) (P=0.1857, Student t-test) (Fig. 4a, b). However, the retention data for diet-fed vectors (Fig. 4b) were significantly different from those for CPmP-1-fed (P=0.0012, Mann–Whitney test) and WT LIYV-fed vectors (P=0.0013, Mann–Whitney test). Correspondingly, virus transmission was observed following the inoculation access feeding of target plants by vectors fed CPmP-1 or WT LIYV preparations. The cumulative transmission scores for CPmP-1 and WT LIYV were 6/20 plants tested and 10/20 plants tested, respectively (Fig. 4b). The difference in transmission was not significant (P=0.3332; Fisher exact test). No transmission was observed for similarly treated diet-fed vectors (Fig. 4b). The presence of the chimeric CPm in CPmP-1 was confirmed by sequencing cloned RT-PCR products containing the CP and CPm sequences generated from the virion RNA of randomly selected CPmP-1 preparations (data not shown).

Virion preparations of CPmP-2 (at concentrations ranging from 52 to 107 ng μl^{-1}), CPmP-3 (61–112 ng μl^{-1}) and CPmP-4 (312–520 ng μl^{-1}) were each tested in two (for CPmP-2 and CPmP-3) or three (for CPmP-4) biological repeat VRT assays, along with WT LIYV preparations and diet-only controls. In the VR assays, fluorescent signals were observed in the foreguts of an average of 2.5 (based on a cumulative total of 16/633), 2.8 (based on a cumulative total of 18/643) and 3.6% (based on a cumulative total of 35/972) of the whiteflies that fed on the preparations of CPmP-2, CPmP-3 and CPmP-4, respectively (Fig. 4a, b). The retention scores for vectors that fed WT LIYV preparations (Fig. 4b) were significantly higher compared to those fed preparations of CPmP-2 (P=0.0002, Mann–Whitney test), CPmP-3 (P=0.0002, Mann–Whitney test) and CPmP-4 (P<0.00001; Mann–Whitney test). Correspondingly, no transmission was observed following the inoculation access feeding of target plants by vectors fed CPmP-2, -3, or -4 preparations, with cumulative scores of 0/8, 0/8 and 0/12 plants tested, respectively (Fig. 4b). In contrast, transmission was observed when vectors fed WT LIYV preparations were given inoculation access on target plants, with cumulative scores of 5/8, 4/8 and 7/12 plants tested compared to those of CPmP-2, -3, and -4, respectively (Fig. 4b).

The chimeric CPm of CPmP-1 is incorporated into virions retained in the vector's foregut

The whitefly transmissibility of CPmP-1, and its ability to retain in the vector's foregut, led to the intriguing hypotheses that a chimeric LIYV CPm consisting of 60% (291 out of 485 amino acids) of the LCV CPm at its proximal (N-terminal) end could be – (1) stably incorporated into LIYV virions and (2) mediate their retention in the vector's foregut. To test the first hypothesis, we first performed IGL-TEM analyses on the virion preparations of CPmP-1, along with that of the following controls: WT LIYV, WT

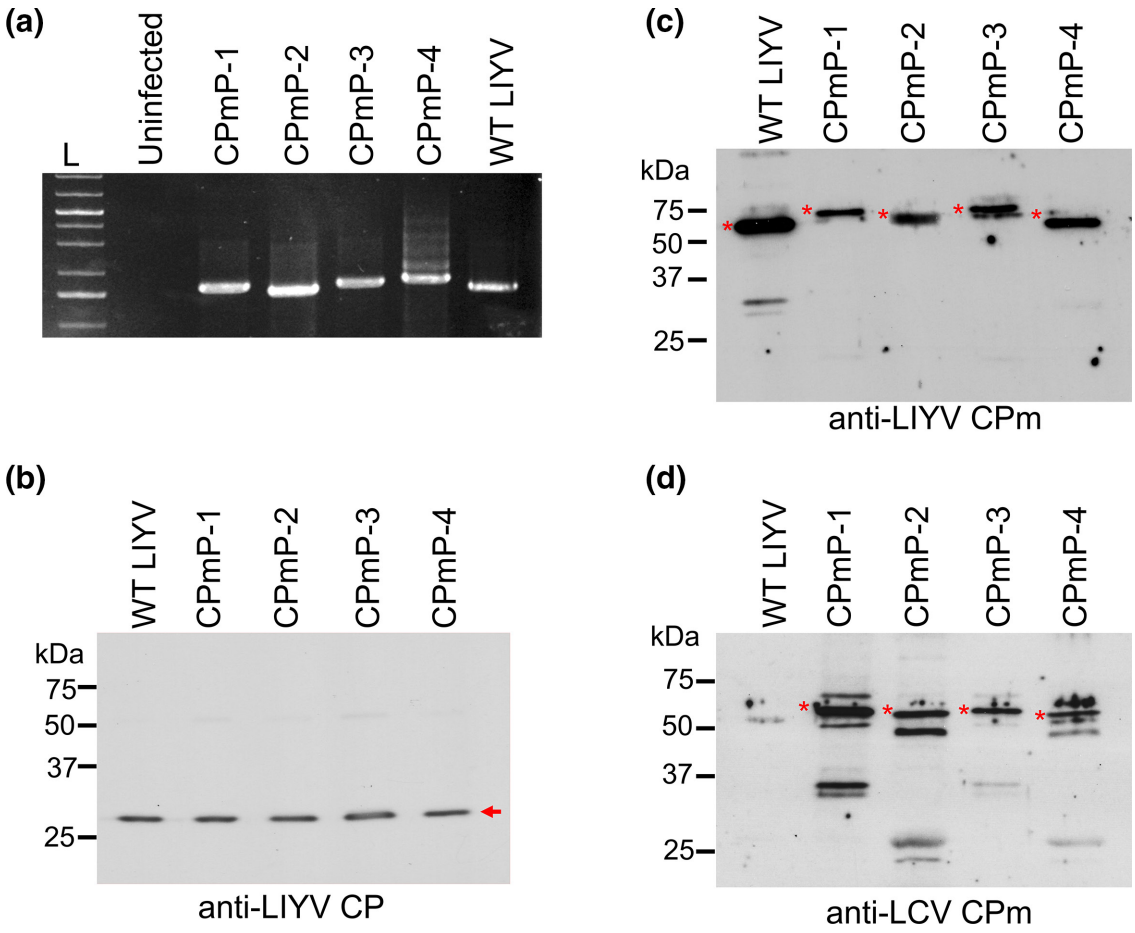

Fig. 3. Systemic infectivity of LIYV CPmP mutants in *Nicotiana benthamiana* plants determined using reverse transcription (RT)-PCR and immunoblot analyses. (a) A representative ethidium bromide-stained agarose gel showing the RT-PCR products obtained using the total RNA of newly emerged (systemic) leaves of uninfected *N. benthamiana* plants and those agroinfiltrated with the binary plasmid constructs of WT LIYV or CPmP mutants. PCR amplification was performed using primers flanking the CPm region. The expected sizes of the PCR products obtained from the CPmP-1, CPmP-2, CPmP-3, CPmP-4 and WT LIYV samples were 1588, 1471, 1582, 1656 and 1486 bp, respectively. L, 1 kb plus DNA ladder. (b–d) The systemic leaves that tested positive for each of the viruses were harvested for virion purification and the resulting preparations were analysed by immunoblots using antibodies produced against LIYV CP (b), LIYV CPm (c), or LCV CPm (d). The molecular masses of protein standards are shown to the left of each blot. The position of the LIYV CP (28 kDa) is indicated by a red arrow. The asterisks mark the positions of the expected molecular masses of WT LIYV CPm (52 kDa) and the chimeric CPm of CPmP-1 (55.6 kDa), CPmP-2 (51.2 kDa), CPmP-3 (55 kDa) and CPmP-4 (51 kDa). The presence of proteins with molecular masses that are lower than that of the CPm identified in (c) and (d) could be the products of protein degradation [9, 44].

LCV and the *B. tabaci* NW non-transmissible CPmP-4, using the antibodies directed against each of the following antigens: LIYV CP, LIYV CPm, LCV CP and LCV CPm. An examination of the electron micrographs revealed that the CPmP-1 and CPmP-4 particles were mostly indistinguishable, by length and morphology, from those of WT LIYV (Fig. 5a–l). With respect to immuno-gold labelling, the anti-LIYV CP antibody positively labelled virtually the entire 'body' length of the CPmP-1 and CPmP-4 particles (Fig. 5a, e). This was expected since, like WT LIYV (Fig. 5i), the chimeric CPmP mutants were engineered in the LIYV RNA 2 background (with a WT LIYV CP ORF). Interestingly, the anti-LIYV CPm antibody, which identified the chimeric CPm of CPmP-1 and CPmP-4 in immunoblot analyses (Fig. 3), could not identify its target antigen on these virus particles as no gold labelling was observed (Fig. 5b, f); unlike with WT LIYV, where labelling was observed on one end of the particles (Fig. 5j). No labelling was observed on the negative control (LCV) particles tested using both the anti-LIYV CP and the anti-LIYV CPm antibodies (Fig. 5m, n). As expected, the anti-LCV CP antibody could not identify its target on the CPmP-1, CPmP-4 and WT LIYV particles (Fig. 5c, g and k); unlike with the WT LCV particle seen in Fig. 5o, where labelling was seen along nearly its entire 'body' length. While the anti-LCV CPm antibody also could not identify its target on the CPmP-4 and WT LIYV particles, labelling of one end of the CPmP-1 particles was clearly observed in many instances (Fig. 5d, h and l), similar to what was observed for WT LCV (Fig. 5p). The labelling of CPmP-1, but not CPmP-4, particles by the

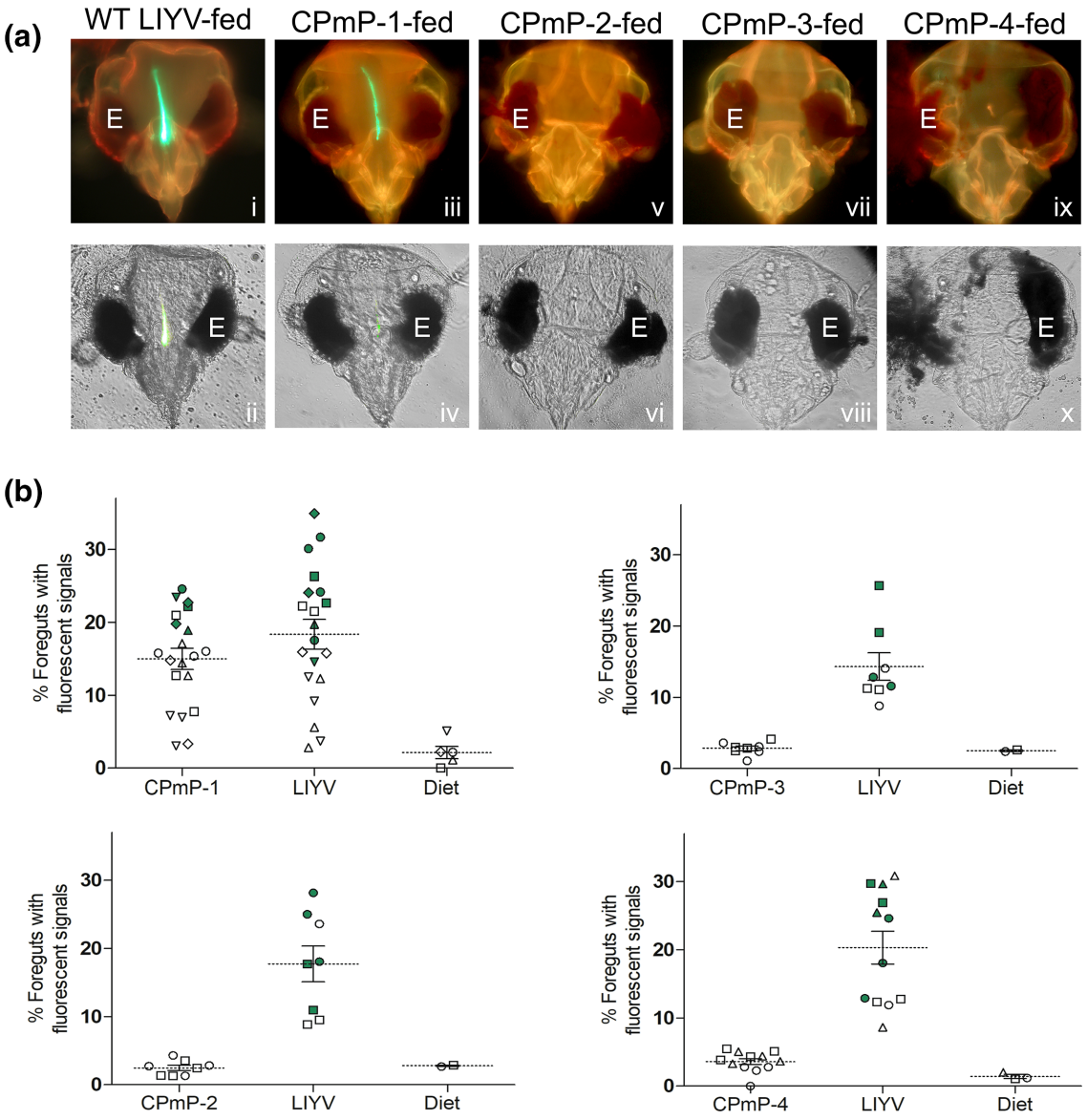

Fig. 4. Virus retention and transmission (VRT) assays of chimeric CPmP mutants using vector whitefly, *B. tabaci* NW. Caged whiteflies (approx. 250 per cage) were fed artificial diet alone or artificial diet containing the virion preparation of each of the following: WT LIYV, chimeric CPmP mutants CPmP-1, CPmP-2, CPmP-3 and CPmP-4. Following acquisition feeding, the whiteflies from each cage were separated into two approximately equal groups. The first group was subjected to retention (VR) assays, while the second group was transferred to a target lettuce plant to determine virus transmissibility. Virus retention was determined by immunofluorescent localization, where whiteflies were essentially fed artificial diet containing anti-virion antibodies, followed by artificial diet containing goat anti-rabbit IgG conjugated with Alexa Fluor 488, with two clearing (diet feeding alone) steps – one before and one after both the antibody-feeding steps. Following the feeding, the heads of the whiteflies were dissected and examined using widefield fluorescence microscopy. (a) Representative images of the dissected heads of whiteflies. Images were taken with transmitted white light blocked (i, iii, v, vii and ix) and unblocked (ii, iv, vi, viii and x). E, whitefly's eye. (b) Graphs showing the VRT results for WT LIYV and each of the chimeric CPmP mutants. Each data point indicates the percentage (%) of foreguts with fluorescent signals for an independent cage (a technical replicate of approx. 125 foreguts) within 1 experiment (a biological repeat). Symbols (circles, squares, diamonds, upright triangles, or upside-down triangles) represent different biological repeats. Means (dashed lines) and standard errors (solid lines) are indicated. Virus transmissibility for each cage was determined by scoring the target plant as either infected (green symbol) or not infected (clear symbol).

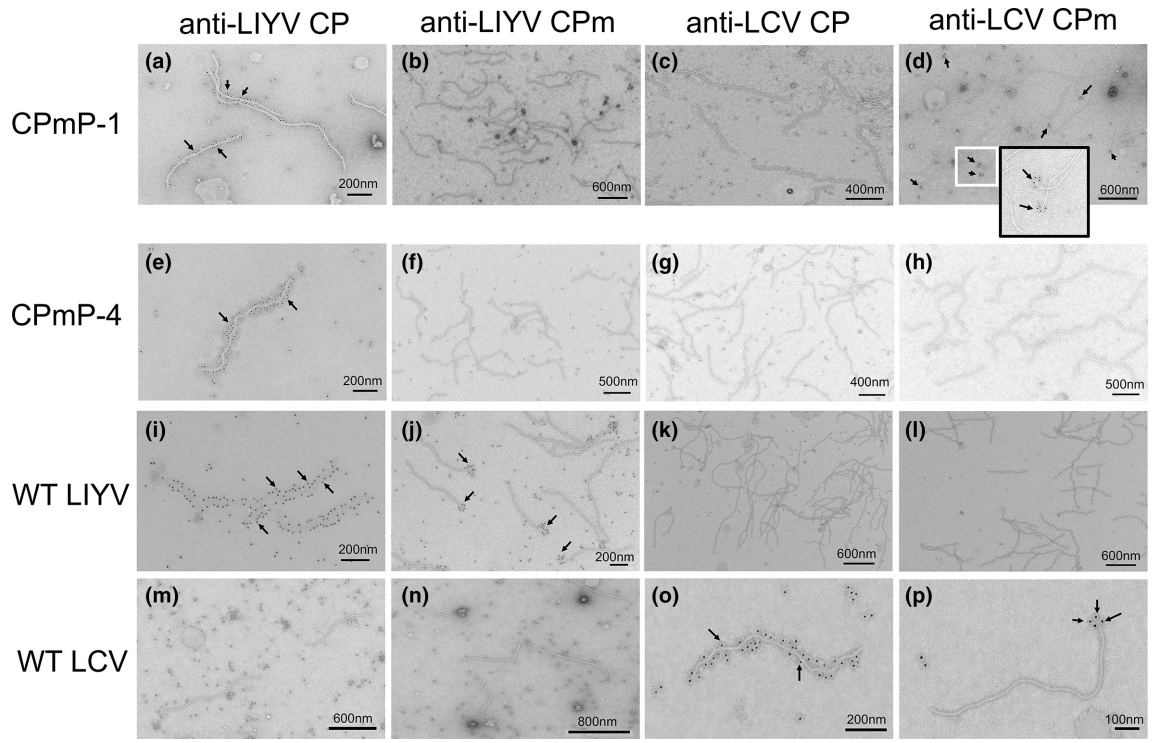

Fig. 5. Immuno-gold labeling-transmission electron microscopy (IGL-TEM) analysis of virion preparations. The particles of LIYV mutants with chimeric partial-length LCV CPm – CPmP-1 (a–d), CPmP-4 (e–h), WT LIYV (i–l) and WT LCV (m–p) – were purified from the systemic leaves of *N. benthamiana* plants infected with the respective viruses. IGL-TEM analyses of the purified preparations were performed using the antibodies against the LIYV CP (a, e, i, m), LIYV CPm (b, f, j, n), LCV CP (c, g, k, o) and LCV CPm (d, h, l, p). In (d), the black-framed box that extends out of the image contains an enlarged view of the selected area identified by the white-framed box within the image. Arrows indicate the sites labelled with gold particles. Scale bars representing lengths in nanometers (nm) are shown in each image.

anti-LCV CPm antibody was noteworthy, given that the same antibody successfully identified the chimeric CPm of both mutants in immunoblot analyses (Fig. 3). Since CPmP-2 and CPmP-3 were like CPmP-4 in that they were also foregut retention- and transmission-defective, additional IGL-TEM experiments were conducted to determine if they exhibited the same gold-labelling patterns as CPmP-4. As expected for both mutants, immunogold-labelling (using anti-LIYV CP antibodies) was observed throughout almost the entire the entire length of the virus particles. As with CPmP-4, none of the CPmP-2 and -3 particles were labelled with either anti-LCV CP or anti-LCV CPm antibodies (Fig. S2). With anti-LIYV CPm antibodies, gold-labelling was observed at one end of the CPmP-2 and -3 particles. However, only relatively few particles were labelled (Fig. S2) and the labelling appeared to be sparsely distributed and less intense compared with those typically observed on WT LIYV particles.

To test the second hypothesis that the chimeric CPm of CPmP-1 would mediate virion retention in the vector's foregut, and to possibly determine which region(s) of the chimeric CPm was involved in mediating this process, we performed VR assays in which whiteflies fed diet containing purified CPmP-1 virions or WT LIYV virions were tested for the presence of the virus in their foreguts using the anti-LIYV CPm or anti-LCV CPm antibodies. When anti-LIYV CPm antibody was used, fluorescent signals were observed in the vectors that fed on WT LIYV virions (at 812 ng μl^{-1}) (Fig. 6a), with 14.6% of the foreguts (a cumulative total of 28/192) examined showing signals (Fig. 6b). In contrast, only 2.3% (a cumulative total of 5/215) of the vectors that fed on CPmP-1 virions (at 523 ng μl^{-1}) contained fluorescent signals in their foreguts, and this was significantly lower than was observed in WT LIYV-fed whiteflies (P=0.0006, Student t-test) (Fig. 6a, b). Remarkably, when the anti-LCV CPm antibody was used, fluorescent signals were observed in the foreguts of 18.5% (a cumulative total of 40/216) of the CPmP-1-fed vectors, and this was significantly higher than the 3.2% (a cumulative total of 7/215) of WT LIYV-fed vectors that contained fluorescent signals in their foreguts (P=0.0002, Student t-test) (Fig. 6a, b).

Taken together, the VR results here (Fig. 6), consistent with those for the IGL-TEM analyses shown in Fig. 5, strongly suggested that the chimeric CPm, containing partial-length LCV CPm and LIYV CPm, was incorporated in the foregut-bound CPmP-1 virions in a manner that allowed its identification by the anti-LCV CPm antibody, but not by the anti-LIYV CPm antibody, under non-denaturing (VR and IGL-TEM) conditions.

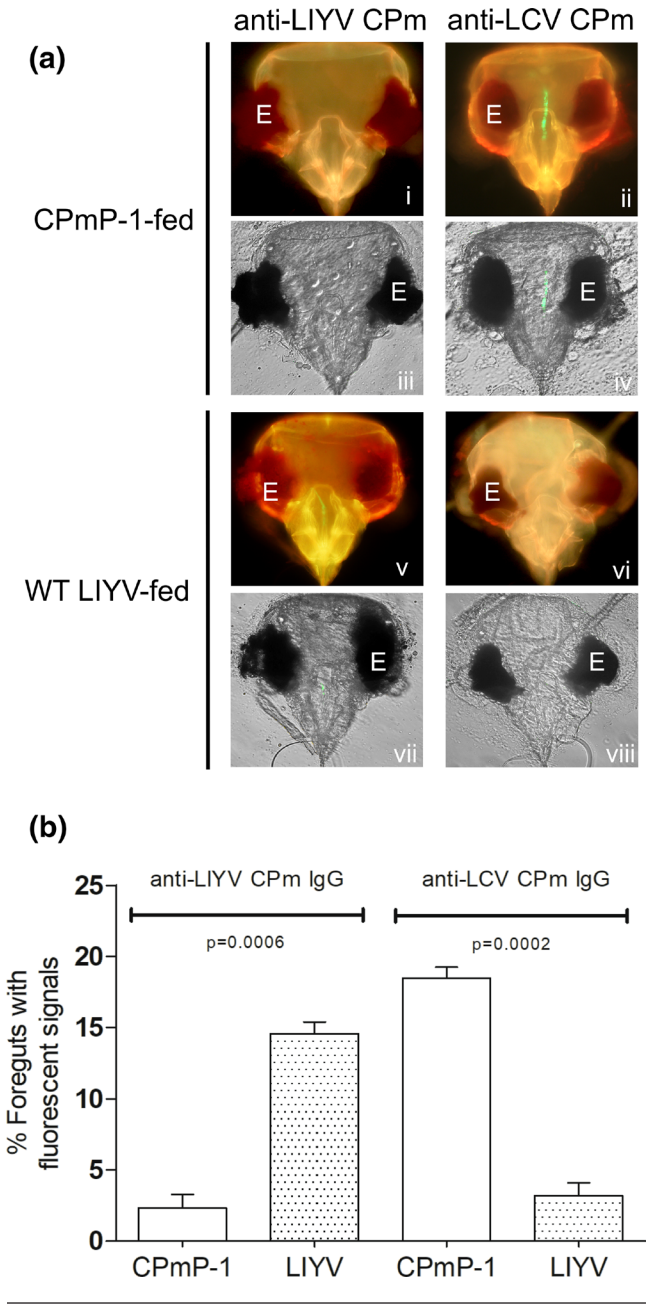

Fig. 6. Virus retention assays of CPmP-1 and WT LIYV in the foreguts of vector whiteflies using antibodies directed against the LIYV CPm or LCV CPm. Caged whiteflies were sequentially fed artificial diet containing the following: (1) WT LIYV or CPmP-1 virions, (2) anti-LIYV CPm or anti-LCV CPm antibodies and (3) goat anti-rabbit IgG conjugated with Alexa Fluor 488, with two clearing steps as described in the Fig. 4 legend. Following feeding, the heads of the whiteflies were dissected and examined using widefield fluorescence microscopy. (a) Representative images of the dissected heads of whiteflies, with transmitted white light blocked (i, ii, v and vi) and unblocked (iii, iv, vii and viii). E, whitefly's eye. (b) The average percentage of CPmP-1-fed and WT LIYV-fed vector whiteflies with fluorescent signals observed in their foreguts determined using anti-LIYV CPm or anti-LCV CPm antibodies in step 3 of the sequential feeding procedure. The results, determined from three technical replicates, were analysed by Student *t*-test to determine the *P* values (as indicated). Error bars represent standard error (SE).

DISCUSSION

LIYV is a definitive example of a virus that, as part of its transmission repertoire, binds to the foregut of its insect vector using a capsid strategy involving a minor capsid component, i.e. the CPm [4, 6]. However, little is known about the structural and functional features of LIYV CPm that facilitate its interaction with the vector. Using bioinformatics involving protein prediction analyses of the CPm, our results indicate a modest but interesting similarity between the proximal one-third (N-terminus) region of LCV CPm (and the CPm of other criniviruses) and both α1LG4-5 and α2LG4-5. It is unclear why the analyses of LIYV CPm did not identify any laminin subunits, but apparently the homology between LIYV CPm and laminin is below detectable thresholds. Members of the laminin family are ubiquitous in many living organisms and are responsible for important common and specific biological functions. In vertebrates and other bilaterians, laminins undergo polymerization to build a network that forms part of the basement membrane [28], and play an important role in providing morphogenetic cues to epithelial cells by interacting with/adhering to cellular receptors, such as integrin, dystroglycan and heparin, as well as sulfated glycolipids that are anchored in the plasma membrane of cells located adjacent to basement membranes [29–31]. During the embryogenesis of model bilaterians (fly, worm and mammals), laminins are involved in cell polarization, a fundamental process associated with cell differentiation and organization [31, 32]. The binding of a phytopathogenic protozoan, *Phytomonas serpens*, to the salivary gland of its insect vector, *Oncopeltus fasciatus* (the large milkweed bug), has been shown to be associated with its interaction with a laminin-like salivary gland protein [33]. Interestingly, the helper-component protease, a viral encoded transmission factor that mediates virion binding of tobacco etch virus to its aphid vector, was found to interact with an aphid ribosomal protein homologous to a laminin precursor [34]. High-affinity laminin-binding receptor proteins on insect and mammalian cells have also been shown to play a role in mediating the binding and entry of a number of viruses [35–38]. Our bioinformatics studies suggested that the proximal (N-terminal) one-third (LCV CPm) region of the chimeric CPm might be involved in ligand binding and prompted the work on the chimeric CPmP mutants. In addition, the amino acid sequence of the LIYV CP preferentially aligns with the distal (C-terminal) one-half of the CPm sequences of other criniviruses (Fig. 2b), and three amino acid residues – S, R, and D – are invariant in all filamentous coat proteins [26] and found in that region. These observations raised the possibilities that while the CPm plays a structural role in the 'tail' assembly of the virion [39], its N-terminal region, in particular, may be involved in virion retention within the vector's foregut.

Using cloned LIYV RNA 2-based cDNA constructs engineered to heterologously encode chimeric partial-length LCV CPm (CPmP) mutants, we have gained further insights into the role of the CPm in encapsidation and the mediation of virion retention and transmission by NW vectors. Two significant results have emerged from these chimeric CPmP

mutant studies. First, outcomes from agroinfiltration studies of the CPmP mutants have added new evidence corroborating the dispensability of the cognate LIYV CPm for systemic infection deduced previously from studies of 1-5b and other unpublished observations [9, 40]. Second, while all four mutants systemically infected agroinoculated *N. benthamiana* plants and expressed the expected chimeric CPms, three were defective in retention and transmission; only one, CPmP-1, could be retained in the vectors' foreguts and transmitted at levels comparable to that of WT LIYV. The presence of the chimeric CPm in CPmP-1 was confirmed by immunoblot analysis (Fig. 3c, d) and by nucleotide sequencing. The transmission and retention results for CPmP-1 are consistent with the hypothesis that region(s) spanning the N-terminal one-half (amino acid position 17 to 292) (Fig. 2a), encoded by genomic regions 1 and 2 (Fig. 1b), of the LCV CPm could be involved in ligand binding in the vector's foregut. Interestingly, a Phyre[2] bioinformatics search using the LCV CPm sequence yielded some rather compelling results (Table S3). With relatively high confidence (88 and 83%), the watermelon mosaic potyvirus CP aligned with the C-terminal region and Con-A family of lectins aligned to the N-terminal region. The next two significant hits were with another potyvirus and lectin (71 and 59%, respectively). This is consistent with a model of a possible bifunctional nature of CPm where the N-terminus is involved with receptor adhesion and the C-terminus forms the RNA binding coat protein. Amino acid position 208–292 (the unstructured/random coil region) (Fig. 2a), encoded by genomic region 2 (Fig. 1b), of the LCV CPm does not share any structural homology with known proteins. However, unstructured regions are known to confer structural plasticity to proteins and maximize their contacts with ligands over a large binding surface and allow binding to multiple targets [41, 42]. Indeed, this unstructured region of LCV CPm appeared to be very important, since when totally (CPmP-2) or partially (CPmP-3) eliminated (Fig. 1b), virus retention and transmission were compromised, even if the hypothesized ligand binding proximal (N-terminal) one-third region (amino acid position 17–181) of the LCV CPm was present (Fig. 4). Studies of the CPmP-4 mutant showed that the arrangement of the chimeric CPm is also important for functionality. Placing the partial-length LIYV CPm, containing regions 1 and 2 (the 46 amino acid unstructured region), in the proximal (N-terminal) one-half, and the partial-length LCV CPm, containing region 3, in the distal (C-terminal) one-half of the chimeric CPm (Fig. 1b), resulted in defective retention and transmission by the vector.

The immunoblot analysis of CPmP-4 (Fig. 3) demonstrated that the chimeric CPm was expressed in infected *N. benthamiana* plants and was present in the virus preparation. Notwithstanding, it is possible that the chimeric CPm was not incorporated into virus particles or was incorporated in a manner that did not result in positive labelling in IGL-TEM (Fig. 5f, h). In the case of CPmP-2 and CPmP-3, both mutants encode the C-terminal one-third of the LIYV CPm (like that of CPmP-1). In addition, virus particles were labelled using anti-LIYV CPm antibodies, albeit weakly and few in numbers (Fig. S2), and the basis underlying this phenomenon remained unclear. In light of this observation, we cannot rule out the possibility that their chimeric CPms were incorporated into virus particles, although they could be present in a manner that differed from that of CPmP-1. One potential consequence of this difference is that, unlike CPmP-1, CPmP-2 and -3 failed to be recognized by anti-LCV CPm antibodies in IGL-TEM and are defective in foregut binding and transmission by NW vectors.

What is unequivocal and particularly unique about CPmP-1 is the propensity of its chimeric CPm to be incorporated into infectious, foregut-binding and transmissible virions, even though it is not clear how this is achieved. Data from the IGL-TEM and VR assays of CPmP-1 virions using anti-LCV CPm antibody clearly showed that the chimeric CPm was incorporated in the capsid in an orientation or conformation that allowed the LCV CPm region to be recognized by the antibody. In contrast, the same assays performed using the anti-LIYV CPm antibody could not identify the LIYV CPm region of the chimeric CPm (Figs 5 and 6). Yet, both antibodies identified their chimeric CPm targets under the denaturing condition of SDS polyacrylamide gel electrophoresis and immunoblot analysis (Fig. 3). The corollary of these observations is that the native form of the chimeric CPm may be incorporated in the assembled virion in a conformation that exposes the N-terminal (LCV CPm) region, thus allowing it to be accessible by the anti-LCV CPm antibody in non-denaturing assays. In comparison, the C-terminal (LIYV CPm) region may not be exposed on the surface of the protein and is therefore not accessible by the anti-LIYV CPm antibody.

The retention and transmission of CPmP-1 virions could not have been mediated by the other three capsid components, i.e. CP, HSP70h and p59. Our previous immunofluorescent localization assays already demonstrated that the percentages of vector foreguts that retained fluorescent signals following the acquisition feeding of *E. coli* expressed recombinant CP, HSP70h and p59 were negligible compared to the diet-fed controls [4]. Furthermore, had these capsid proteins supported virion retention and transmission, fluorescent signals in a significant (WT level) number of vectors' foreguts and infection of the target plants would have been observed following the acquisition and inoculation feeding of one or more of the other three chimeric CPm mutants (CPmP-2, -3 and -4). Instead, only CPmP-1 exhibited similar retention and transmission to WT LIYV.

Although the concentrations of mutants CPmP-1–4 were lower than that of the WT, it is unlikely that they contributed to the defect in virion retention and transmission. If these concentration levels had impacted negatively on the transmission process, a range of levels of retention and transmission would have been observed in all four mutants, as opposed to the WT levels of retention and transmission seen in CPmP-1, and the insignificant retention (similar to that seen in the diet-fed vectors) and complete absence of virus transmission in CPmP-2, -3 and -4 (Fig. 4). In addition, our previous study

[20] had shown that WT LIYV could be transmitted by NW vectors efficiently at a virion concentration of 10 ng μl^{-1} under similar experimental conditions to those of the present study. The lowest and highest concentrations of the retention and transmission defective mutants, 52 (for CPmP-2) and 520 ng μl^{-1} (for CPmP-4), respectively, were more than 5- and 50-fold higher than 10 ng μl^{-1}.

Because LCV and LIYV are both transmissible by *B. tabaci* NW [43, 44], the positive identification of the chimeric CPm (by the anti-LCV CPm antibody) in the immuno-based VR and IGL-TEM studies of the whitefly transmissible CPmP-1 does not in any way imply that virion retention and transmission are conferred solely by the LCV CPm portion of the chimeric CPm. However, since the LCV CPm region of CPmP-1 virions is potentially exposed on the surface of the chimeric CPm, it is possible that the N-terminal region, or part thereof, is in contact with the foregut retention site. Although the LIYV CPm does not appear to be accessible to the anti-LIYV CPm antibody, we cannot rule out its participation in these functions; it must be involved in encapsidation of the chimeric CPm, which is a prerequisite for virion retention and transmission. The availability of a functional CPm mutant, CPmP-1, would allow us to gain new insights into the mechanism of crinivirus transmission, such as determining the vector-specific transmission of CPmP-1 by *B. tabaci* MEAM 1, a vector of LCV but not LIYV [43, 44]. Such an investigation would require the testing of control constructs of chimeric LIYV CPm–LCV CPm engineered in the infectious clone of LCV RNA 2.

The results of this study provide new evidence showing the structural plasticity of the LIYV CPm. It is able to accommodate a substantial portion of the CPm of the related LCV to result in a functional hybrid CPm that is incorporated in the virion. These results demonstrate that it will be possible to perform further mapping studies to identify determinants on the LIYV/LCV CPm that mediate virion retention and transmission by whitefly vectors.

Funding information
Funds supporting this work were provided by a grant from the National Science Foundation (#1146797) and, in part, by a grant (RGP0013/2015) from the Human Frontier Science Program, awarded to J.C.K.N.

Acknowledgements
We thank Nuttawat Yongpairojwong for technical assistance.

Author contributions
J.N.: conceptualization, methodology, writing – original draft, writing – review and editing, supervision, project administration, funding acquisition. J.P.: conceptualization, methodology, investigation. A.C.: methodology, investigation, writing – original draft. T.T.: investigation. J.Z.: formal analysis. T.S.: conceptualization, writing – review and editing.

Conflicts of interest
The authors declare that there are no conflicts of interest

References

1. Ng JCK, Zhou JS. Insect vector-plant virus interactions associated with non-circulative, semi-persistent transmission: Current perspectives and future challenges. *Curr Opin Virol* 2015;15:48–55.
2. Karasev AV. Genetic diversity and evolution of closteroviruses. *Annu Rev Phytopathol* 2000;38:293–324.
3. Yeh HH, Tian T, Rubio L, Crawford B, Falk BW. Asynchronous accumulation of lettuce infectious yellows virus RNAs 1 and 2 and identification of an RNA 1 trans enhancer of RNA 2 accumulation. *J Virol* 2000;74:5762–5768.
4. Chen AYS, Walker GP, Carter D, Ng JCK. A virus capsid component mediates virion retention and transmission by its insect vector. *Proc Natl Acad Sci U S A* 2011;108:16777–16782.
5. Medina V, Sudarshana MR, Tian T, Ralston KS, Yeh H-H, *et al*. The lettuce infectious yellows virus (LIYV)-encoded P26 is associated with plasmalemma deposits within LIYV-infected cells. *Virology* 2005;333:367–373.
6. Ng J. A quantum dot-Immunofluorescent labeling method to investigate the interactions between a crinivirus and its whitefly vector. *Front Microbiol, Methods* 2013;4.
7. Qiao W, Medina V, Kuo YW, Falk BW. A distinct, non-virion plant virus movement protein encoded by a crinivirus essential for systemic infection. *mBio* 2018;9.
8. Stewart LR, Medina V, Sudarshana MR, Falk BW. Lettuce infectious yellows virus-encoded P26 induces plasmalemma deposit cytopathology. *Virology* 2009;388:212–220.
9. Stewart LR, Medina V, Tian T, Turina M, Falk BW, *et al*. A mutation in the lettuce infectious yellows virus minor coat protein disrupts whitefly transmission but not in planta systemic movement. *J Virol* 2010;84:12165–12173.
10. Tian TY, Rubio L, Yeh HH, Crawford B, Falk BW. *Lettuce infectious yellows virus*: in vitro acquisition analysis using partially purified virions and the whitefly *Bemisia tabaci*. *J Gen Virol* 1999;80:1111–1117.
11. Liu H-Y, Wisler GC, Duffus JE. Particle lengths of whitefly-transmitted criniviruses. *Plant Dis* 2000;84:803–805.
12. Peremyslov VV, Andreev IA, Prokhnevsky AI, Duncan GH, Taliansky ME. Complex molecular architecture of beet yellows virus particles. *Proc Natl Acad Sci U S A* 2004;101:5030–5035.
13. Satyanarayana T, Gowda S, Ayllón MA, Dawson WO. Closterovirus bipolar virion: evidence for initiation of assembly by minor coat protein and its restriction to the genomic RNA 5′ region. *Proc Natl Acad Sci U S A* 2004;101:799–804.
14. Li J, Liang X, Wang X, Shi Y, Gu Q, *et al*. Direct evidence for the semipersistent transmission of Cucurbit chlorotic yellows virus by a whitefly vector. *Sci Rep* 2016;6:36604.
15. Waterhouse A, Bertoni M, Bienert S, Studer G, Tauriello G. SWISS-MODEL: homology modelling of protein structures and complexes. *Nucleic Acids Res* 2018;46:W296–W303.
16. Kelley LA, Mezulis S, Yates CM, Wass MN, Sternberg MJE. The Phyre2 web portal for protein modeling, prediction and analysis. *Nat Protoc* 2015;10:845–858.
17. Garnier J, Gibrat JF, Robson B. GOR method for predicting protein secondary structure from amino acid sequence. *Methods Enzymol* 1996;266:540–553.
18. Wang J, Turina M, Stewart LR, Lindbo JA, Falk BW. Agroinoculation of the *Crinivirus*, *Lettuce infectious yellows virus*, for systemic plant infection. *Virology* 2009;392:131–136.
19. Chen AYS, Pavitrin A, JCK N. Agroinoculation of the cloned infectious cDNAs of *Lettuce chlorosis virus* results in systemic plant infection and production of whitefly transmissible virions. *Virus Res* 2012;169:310–315.
20. Ng JCK, Tian T, Falk BW. Quantitative parameters determining whitefly (*Bemisia tabaci*) transmission of Lettuce infectious yellows virus and an engineered defective RNA. *J Gen Virol* 2004;85:2697–2707.
21. Ng JCK, Falk BW. Bemisia tabaci transmission of specific Lettuce infectious yellows virus genotypes derived from in vitro synthesized transcript-inoculated protoplasts. *Virology* 2006;352:209–215.
22. Agirrezabala X, Méndez-López E, Lasso G, Sánchez-Pina MA, Aranda M. The near-atomic cryoEM structure of a flexible filamentous

plant virus shows homology of its coat protein with nucleoproteins of animal viruses. *Elife* 2015;4:e11795.

23. Harrison D, Hussain S-A, Combs AC, Ervasti JM, Yurchenco PD, *et al*. Crystal structure and cell surface anchorage sites of laminin α1LG4-5. *J Biol Chem* 2007;282:11573–11581.
24. Fahey B, Degnan BM. Origin and evolution of laminin gene family diversity. *Mol Biol Evol* 2012;29:1823–1836.
25. Tisi D, Talts JF, Timpl R, Hohenester E. Structure of the C-terminal laminin G-like domain pair of the laminin α2 chain harbouring binding sites for α-dystroglycan and heparin. *EMBO J* 2000;19:1432–1440.
26. Dolja VV, Boyko VP, Agranovsky AA, Koonin EV. Phylogeny of capsid proteins of rod-shaped and filamentous RNA plant viruses: two families with distict patterns of sequence and probably structure conservation. *Virology* 1991;184:79–86.
27. Klaassen VA, Boeshore ML, Koonin EV, Tian TY, Falk BW. Genome structure and phylogenetic analysis of lettuce infectious yellows virus, a whitefly-transmitted, bipartite closterovirus. *Virology* 1995;208:99–110.
28. Henrikson RC, Kaye GI, Mazurkiewicz JE. *National Medical Series for Independent Study*. 1st edn. Baltimore: Lippincott Williams & Wilkins; 1997.
29. Aumailley M. The laminin family. *Cell Adh Migr* 2013;7:48–55.
30. Talts JF, Andac Z, Göhring W, Brancaccio A, Timpl R. Binding of the G domains of laminin α1 and α2 chains and perlecan to heparin, sulfatides, α-dystroglycan and several extracellular matrix proteins. *EMBO J* 1999;18:863–870.
31. Li S, Edgar D, Fässler R, Wadsworth W, Yurchenco PD. The role of laminin in embryonic cell polarization and tissue organization. *Dev Cell* 2003;4:613–624.
32. Miner JH. Laminins and their roles in mammals. *Microsc Res Tech* 2008;71:349–356.
33. de Almeida Dias F, Souza dos Santos AL, Santos Lery LM, Alves e Silva TL, Oliveira MM, *et al*. Evidence that a laminin-like insect protein mediates early events in the interaction of a Phytoparasite with its vector's salivary gland. *PLoS One* 2012;7:e48170.
34. Fernández-Calvino L, Goytia E, López-Abella D, Giner A, Urizarna M. The helper-component protease transmission factor of tobacco etch potyvirus binds specifically to an aphid ribosomal protein homologous to the laminin receptor precursor. *J Gen Virol* 2010;91:2862–2873.
35. Sakoonwatanyoo P, Boonsanay V, Smith DR. Growth and production of the dengue virus in C6/36 cells and identification of a laminin-binding protein as a candidate serotype 3 and 4 receptor protein. *Intervirology* 2006;49:161–172.
36. Wang KS, Kuhn RJ, Strauss EG, Ou S, Strauss JH. High-affinity laminin receptor is a receptor for sindbis virus in mammalian cells. *J Virol* 1992;66:4992–5001.
37. Chen J, WR H, Shen L, Dong H, Yu J. The laminin receptor is a cellular attachment receptor for classical Swine Fever virus. *J Virol* 2015;89:4894–4906.
38. Cruz-Oliveira C, Freire JM, Conceição TM, Higa LM, Castanho MA. Receptors and routes of dengue virus entry into the host cells. *FEMS Microbiol Rev* 2015;39:155–170.
39. Alzhanova DV, Prokhnevsky AI, Peremyslov VV, Dolja VV. Virion tails of *Beet yellows virus*: coordinated assembly by three structural proteins. *Virology* 2007;359:220–226.
40. Kiss Z, Medina V, Falk B. Crinivirus replication and host interactions. *Front Microbiol, Review* 2013;4.
41. Miller M. The importance of being flexible: the case of basic region leucine zipper transcriptional regulators. *Curr Protein Pept Sci* 2009;10:244–269.
42. Dyson HJ, Wright PE. Intrinsically unstructured proteins and their functions. *Nat Rev Mol Cell Biol* 2005;6:197–208.
43. Tzanetakis IE, Martin RR, Wintermantel WM. Epidemiology of criniviruses: an emerging problem in world agriculture. *Front Microbiol* 2013;4:119.
44. Ng JCK, Chen AYS. Acquisition of Lettuce infectious yellows virus by Bemisia tabaci perturbs the transmission of Lettuce chlorosis virus. *Virus Res* 2011;156:64–71.